Published in final edited form as:

Circ Res. 2016 July 22; 119(3): 434–449. doi:10.1161/CIRCRESAHA.116.308700.

The BMP Antagonist Gremlin 2 Limits Inflammation After Myocardial Infarction

Lehanna N. Sanders[1,2], **John A. Schoenhard**[1,7], **Mohamed A. Saleh**[3,9], **Amrita Mukherjee**[1,8], **Sergey Rhyzov**[4], **William G. McMaster Jr.**[3,5], **Kristof Nolan**[6], **Richard J. Gumina**[1], **Thomas B. Thompson**[6], **Mark A. Magnuson**[9], **David G. Harrison**[3], and **Antonis K. Hatzopoulos**[1,2]

[1]Department of Medicine - Division of Cardiovascular Medicine, Vanderbilt University Medical Center, Nashville, TN, U.S.A

[2]Department of Cell and Developmental Biology, Vanderbilt University Medical Center, Nashville, TN, U.S.A

[3]Department of Medicine - Division of Clinical Pharmacology, Vanderbilt University Medical Center, Nashville, TN, U.S.A

[4]Maine Medical Center Research Institute, Scarborough, ME, U.S.A

[5]Department of Surgery - Division of General Surgery, Vanderbilt University Medical Center, Nashville, TN, U.S.A.

[6]Department of Molecular Genetics, Biochemistry and Microbiology, University of Cincinnati, Cincinnati, OH, U.S.A.

[7]CentraCare Health, St. Cloud, MN, U.S.A

[8]Cincinnati Children's Hospital Medical Center, Cincinnati, OH, U.S.A

[9]Department of Pharmacology and Toxicology, Faculty of Pharmacy, Mansoura University, Mansoura, Egypt

[10]Center for Stem Cell Biology, Vanderbilt University School of Medicine, Nashville, TN, U.S.A

Abstract

Rationale—We have recently shown that the Bone Morphogenetic Protein (BMP) antagonist Gremlin 2 (Grem2) is required for early cardiac development and cardiomyocyte differentiation. Our initial studies discovered that *Grem2* is strongly induced in the adult heart after experimental myocardial infarction (MI). However, the function of Grem2 and BMP signaling inhibitors after cardiac injury is currently unknown.

Objective—To investigate the role of Grem2 during cardiac repair and assess it's potential to improve ventricular function after injury.

Address correspondence to: Dr. Antonis Hatzopoulos, Department of Medicine - Division of Cardiovascular Medicine, Vanderbilt University Medical Center, Nashville, TN 37232-6300, Tel: (615) 936 5529, FAX: (615) 936 4079, antonis.hatzopoulos@vanderbilt.edu.

DISCLOCURES

None.

Methods and Results—Our data show Grem2 is transiently induced after MI in peri-infarct area cardiomyocytes during the inflammatory phase of cardiac tissue repair. By engineering loss- ($Grem2^{-/-}$) and gain- (TG^{Grem2}) of-Grem2-function mice, we discovered that Grem2 controls the magnitude of the inflammatory response and limits infiltration of inflammatory cells in peri-infarct ventricular tissue, improving cardiac function. Excessive inflammation in $Grem2^{-/-}$ mice after MI was due to over-activation of canonical BMP signaling, as proven by the rescue of the inflammatory phenotype through administration of the canonical BMP inhibitor, DMH1. Furthermore, intra-peritoneal administration of Grem2 protein in wild-type mice was sufficient to reduce inflammation after MI. Cellular analyses showed BMP2 acts with TNFα to induce expression of pro-inflammatory proteins in endothelial cells and promote adhesion of leukocytes, whereas Grem2 specifically inhibits the BMP2 effect.

Conclusion—Our results indicate Grem2 provides a molecular barrier that controls the magnitude and extent of inflammatory cell infiltration by suppressing canonical BMP signaling, thereby providing a novel mechanism for limiting the adverse effects of excessive inflammation after MI.

Subject Terms

Myocardial Infarction; Inflammation; Cell Signaling/Signal Transduction; Genetically Altered and Transgenic Models

Keywords

Acute myocardial infarction; inflammation; BMP signaling pathway; Gremlin 2; mouse mutant

INTRODUCTION

Coronary heart disease resulting in myocardial infarction (MI) is the major cause of death in men and women.[1] Each year about 735,000 people in the U.S. have an MI and most suffer irreversible tissue damage, leading to ventricular remodeling, hypertrophy, dilatation, and eventually heart failure (HF).[2] Following MI, the adult heart undergoes a sequence of molecular and cellular events that delineate the different stages of tissue repair. Initially, cardiomyocytes within infarcted myocardium begin to die within minutes after coronary artery occlusion.[3] Toxic products and signals released from dying cells induce endothelial cell adhesion proteins, as well as cytokines and chemokines, to recruit inflammatory cells that remove tissue debris, and activate proteases to degrade extracellular matrix.[4] After debris is cleared, usually within two to three days after MI, the gap is filled with granulation tissue that is composed of proliferating cells, mainly endothelial cells that form new capillaries, and myofibroblasts that secrete collagen and other matrix proteins.[5] Two to three weeks after the original MI, the infarct begins to mature into a dense scar.[6] We have recently demonstrated that canonical Wnt signaling activation after MI attenuates fibrosis and promotes arteriole formation and cardiogenesis, suggesting that developmental pathways, critical for embryonic cardiac development, are re-activated after injury in the adult heart to regulate tissue repair.[7,8]

Bone Morphogenetic Proteins (BMPs) play important roles during various stages of cardiac development,[9] including early cardiogenic differentiation of mesoderm,[10] cardiac tube assembly, looping and jogging,[11] cardiac chamber identity,[12] cardiomyocyte differentiation[13] and cardiac cushion formation.[14] BMP signaling is also induced after ischemic injury in the adult mouse heart and implicated in cardiomyocyte apoptosis during ischemia/reperfusion.[15,16] Histological analyses showed strong induction of Bmp2 in peri-infarct cardiomyocytes,[17] however the exact role of BMP signaling in cardiac tissue repair, or how BMP signaling is regulated after cardiac injury, is not well understood.

BMPs belong to the Transforming Growth Factor β (TGF-β) superfamily of secreted ligands and bind to type I and type II receptors as dimers, leading to phosphorylation and activation of the type I receptor by its type II partner. Activated type I receptors then phosphorylate Smad1/5/8 intracellular proteins, which complex with Smad4 and translocate to the nucleus, where they regulate expression of target genes such as the *Id* family of transcriptional repressors.[18] BMP signaling is modulated in the extracellular space by a large number of secreted, structurally diverse antagonists, such as Chordin, Noggin and members of the DAN family, that bind to BMP ligands and thereby hinder binding to the corresponding receptors.[19,20]

Gremlin 2 (Grem2), also called Protein Related to Dan and Cerberus (PRDC), belongs to the DAN family of BMP antagonists together with its close paralog Gremlin 1, Dan, Dante (or Coco), Cerberus-like 1, Uterine sensitization-associated gene-1 (USAG-1), and Sclerostin.[21–23] Grem2 was first discovered 15 years ago,[21] but its biological function and mechanism of BMP inhibition have remained largely obscure. *Grem2* expression has been detected in the developing spinal cord and lung mesenchyme,[24,25] and Grem2 has been implicated in follicle, neuronal and bone development.[26–28] Grem2 *in vitro* inhibits Bmp2 and Bmp4, but not Tgfβ or Activin.[26] Although several DAN-family members such as Dante and Grem1 have been linked to pulmonary arterial hypertension, chronic kidney disease and cancer,[29–32] little is known about the role of Grem2 in disease.

We recently established that during embryonic development in zebrafish, *grem2* first appears in the pharyngeal mesoderm next to the forming heart tube.[33,34] Loss- and gain-of-function approaches demonstrated that Grem2 is necessary for cardiac tube jogging and looping, cardiac laterality and cardiomyocyte differentiation by suppression of Smad1/5/8 phosphorylation.[34] Moreover, we found that Grem2 promotes differentiation of pluripotent mouse embryonic stem (ES) cells to atrial-like cardiomyocytes.[35] Here, we show that Grem2 is not essential for mouse embryonic development. In the adult heart, we discovered that Grem2 is highly induced in peri-infarct cardiomyocytes at the end of the inflammatory phase after MI. Using genetic gain- and loss-of-Grem2-function models and chemical compounds that inhibit BMPs, we present evidence that Grem2 is necessary and sufficient to modulate the inflammatory response and keep inflammation in check through suppression of canonical BMP signaling. Grem2 levels after MI correlate with functional recovery, suggesting a new strategy to control inflammation of cardiac tissue after acute ischemic injury and improve cardiac function.

METHODS

A complete Methods section is available in the Online Data Supplement.

RESULTS

Grem2 is transiently induced after MI following the initial inflammatory response

To place BMP signaling components within the context of the MI repair process, we analyzed whole mouse heart RNA samples prepared at distinct time points after left anterior descending (LAD) artery ligation, namely at day 0 (baseline, prior to injury), 1, 2, 3, 5, 7 and 21 after MI. Using typical inflammatory gene markers, such as *Il-1β* and *E-selectin*, and markers of granulation tissue formation and fibrosis, such as *Tgfβ1* and *alpha Smooth Muscle Actin* (α*Sma*), we determined that pro-inflammatory genes are induced early and peak at days 1–2 after MI, whereas fibrosis genes are induced at day 5, as expected.[4,6,8] Gene induction of inflammatory genes returned to baseline levels between days 3 to 5, whereas *Tgfβ1* expression returned to baseline at day 21. α*Sma* levels declined, but were still detectable at day 21, reflecting the presence of myofibroblasts during the scar maturation phase (Figure 1A).

Investigation of BMP ligands after MI showed that *Bmp2* is the earliest induced ligand of the BMP family at day 1 with its expression peaking at day 3, a pattern that corresponds to the inflammatory phase of cardiac repair. Previous work documented Bmp2 protein induction takes place primarily in peri-infarct area cardiomyocytes and not recruited immune cells.[17] *Bmp2* is then downregulated to pre-injury levels by day 7 after MI. *Bmp2* suppression coincides with upregulation of *Bmp4*, *Bmp6*, and *Bmp10*, the expression of which starts around day 5 and persists during fibrosis and scar formation (Figure 1B). Consistent with the induction of distinct BMP ligands during different stages after MI, there was an overlapping expression of the BMP signaling target gene *Id2* throughout the repair process (Online Figure IA). In contrast, analysis of BMP signaling antagonists showed minimal changes in their expression levels after MI with the notable exception of *Grem2* that is induced around day 2, peaks at day 5 after MI and returns to pre-injury levels at day 21 (Figure 1C). The *Grem2* induction pattern follows the pattern of *Bmp2* with one-day delay. We did not detect a signal for its close paralog *Grem1* at baseline, or at the tested time points after MI (Online Figure IB). Although Grem2 is the most prominently induced BMP antagonist after MI, absolute expression values indicate that during homeostasis the heart maintains expression of *Dan*, *Sost*, *Twsg1* and *Chordin* which, however are at least 40 (Chordin) to 400 (Dan, Twsg1) times less potent BMP inhibitors than Grem2, or do not bind directly to BMP ligands (Sost) (Online Figure IB).[36,37]

Consistent with the *Bmp2* induction pattern after MI, immunofluorescence (IF) analysis at day 2 post-MI, using antibodies recognizing the phosphorylated, i.e., activated form of Smad1/5/8, demonstrated activation of canonical BMP signaling in endothelial cells in the peri-infarct area and cardiomyocytes at the border zone of the infarcted tissue. In contrast, we did not detect active Smad1/5/8 within ventricular tissue prior to injury (Figure 1D).

In conclusion, our data indicate a bi-phasic pattern of BMP ligand induction after MI, i.e., early upregulation of *Bmp2* expression during the inflammatory phase, followed by a second phase during granulation tissue and scar formation that is dominated by several ligands, including *Bmp4*, *Bmp6*, and *Bmp10*. Conversely, *Grem2* is the prominent BMP antagonist induced after MI with its expression starting at day 2, peaking during the transition from inflammation to granulation tissue formation, and returning to baseline levels during scar formation. Induction of *Bmp2* coincided with activation of canonical/p-Smad BMP signaling in endothelial cells and cardiomyocytes in the peri-infarct area.

Loss of Grem2 leads to an increase of endothelial pro-inflammatory markers after MI

To determine whether Grem2 has a role in cardiac repair, we generated a loss of function (*Grem2*$^{-/-}$) mouse model by deleting most of exon 2 via homologous recombination (Figure 2A; Online Figure II; see also Methods). This approach deleted the entire coding sequence and most of the 3′ untranslated region of the *Grem2* gene, leading to complete loss of Grem2 protein. *Grem2*$^{-/-}$ mice are viable without major structural or physiological defects or apparent differences in heart size, cardiac tissue morphology and cardiac function as compared to *WT* siblings, with the exception of a small increase in heart rate (Online Table I; Online Figure II). Thus, although the *Grem2* expression pattern has been conserved in zebrafish and mouse embryos, where *Grem2* is first expressed in the area of the secondary heart field,[34,35] Grem2 appears to be dispensable for mouse development.

Antibody staining revealed that the robust induction of Grem2 protein after MI takes place primarily in peri-infarct cardiomyocytes (Figure 2B). There was no detected Grem2 in distal areas away from the infarct (data not shown). There was also a complete absence of Grem2 protein in *Grem2*$^{-/-}$ mice, further corroborating their null phenotype (Figure 2B).

In order to test whether the *Grem2* induction following the upregulation of *Bmp2* expression during the inflammatory phase plays a role in inflammation after acute injury, we challenged *Grem2*$^{-/-}$ and *WT* sibling mice with experimental MI by permanent ligation of the LAD coronary artery. We then isolated whole heart RNA at day 0, 2, 7 and 21 after MI and analyzed the expression of pro-inflammatory genes. Our data show that induction of genes encoding endothelial cell membrane proteins implicated in the rolling and adhesion of circulating immune cells to the vascular wall are higher in *Grem2*$^{-/-}$ hearts compared to *WT*s. Specifically, RNA analysis showed that expression of *E-selectin*, *Vcam1*, and *Icam1* are further upregulated compared to *WT* controls at day 2 and 7 after MI; however, their expression decreases at day 21 to levels comparable to *WT* hearts (Figure 2C).

Consistent with the gene induction results, IF analysis of cardiac tissue sections at day 7 after MI revealed that endothelial cells within the infarct and peri-infarct areas stain positively for E-selectin protein in *Grem2*$^{-/-}$ mice, whereas, at this stage, E-selectin is almost undetectable in *WT* controls (Figure 2D). Comparison of chemokine expression such as *Ccl2*, *Il-8*, and *Il-1β* showed, that although chemokines are induced after MI as expected, relative expression levels were comparable between *Grem2*$^{-/-}$ and *WT* mice, except a further 1.7-fold increase of *Ccl2* expression in *Grem2*$^{-/-}$ mice compared to *WT* (Online Figure IIIA). Together, our data show that Grem2 protein induction takes place in the peri-

infarct zone and lack of Grem2 enhances the expression of pro-inflammatory genes in endothelial cells in and around the injury site after MI.

Loss of Grem2 leads to an increase in the magnitude of inflammation

To test whether increased expression of pro-inflammatory makers after MI augments infiltration of immune cells, we isolated hearts at day 5 after MI and analyzed histological sections with an antibody recognizing the leukocyte marker, CD45. The results showed that infiltration of $CD45^+$ cells after MI appeared more abundant in *Grem2*$^{-/-}$ hearts compared to *WT* (Figure 3A). To quantify the increase in inflammatory infiltrate and better characterize the corresponding cells, we prepared single cell suspensions of non-cardiomyocyte cells and conducted flow cytometry using antibodies recognizing various immune cell markers such as CD45, F4/80, Ly6C, Ccr2, Ly6G and CD3.[38–40] As shown in Figure 3B, there was a 3-fold increase in infiltrating inflammatory cells, identified as $CD45^+$ cells, in *Grem2*$^{-/-}$ hearts after MI as compared to *WTs*. Within the $CD45^+$ population, there was a 2–3-fold increase in $Ly6C^{hi}$ cells that represent mostly monocytes (but may also include neutrophils and T-cells that express intermediate levels of Lyc6), neutrophils ($Ly6G^+$), T-cells ($CD3^+$) and macrophages ($F4/80^+$). There was a similar increase in *Grem2*$^{-/-}$ hearts compared to *WTs* of pro-inflammatory $F4/80^+$ macrophages expressing high levels Ly6C ($F4/80^+/Ly6C^{hi}$), the Monocyte chemoattractant protein-1 (MCP-1, or Ccl2) receptor Ccr2 ($F4/80^+/Ccr2^{hi}$), or both ($F4/80^+/Ly6C^{hi}/Ccr2^{hi}$). The gating strategy and representative flow cytometry plots are shown in the Online Figure IV.

Analysis of the initial necrosis area using Triphenyl tetrazolium chloride (TTC) staining 1 day after MI showed that infarct sizes are comparable between *WT* and *Grem2*$^{-/-}$ hearts, suggesting that the observed differences in the inflammatory response are not due to more severe infarcts in *Grem2*$^{-/-}$ mice (Online Figure V). Furthermore, flow cytometry analysis on blood $CD45^+$ cells isolated from *Grem2*$^{-/-}$ and *WT* mice at baseline and 5 days after MI revealed that leukocyte numbers in the blood were not significantly different at baseline. After MI, the number of circulating leukocytes increased after MI as expected,[41] albeit numbers were ~2 times higher in *Grem2*$^{-/-}$ mice, likely because circulating leukocyte numbers correlate with the magnitude of the inflammatory response (Online Figure VI).[42]

Finally, we investigated whether loss of Grem2, besides increased inflammatory cell infiltration, also leads to prolonged inflammation. To this end, we quantified inflammatory cells by flow cytometry at day 14 after MI, a time point when inflammatory cell numbers return close to baseline levels in *WT* mice. Our results showed a dramatic drop in inflammatory cells in *Grem2*$^{-/-}$ mice to levels comparable to *WT* controls (Figure 3C), consistent with the eventual downregulation of cell adhesion molecules in *Grem2*$^{-/-}$ hearts after MI (Figure 2B). Furthermore, molecular analysis indicated an increase in the induction levels of genes encoding proteins involved in the resolution of inflammation such as *Tgfβ1* and *Il-10* in *Grem2*$^{-/-}$ mice compared to *WT* animals, which may account for the clearing of excessive inflammatory cells in *Grem2*$^{-/-}$ cardiac tissue (Figure 3D). Taken together, our results indicate Grem2 is necessary to regulate the magnitude, but not the duration of the inflammatory cell infiltration after MI.

Grem2 overexpression attenuates the inflammatory response after MI

To explore the possibility that Grem2 controls the extent of inflammation after MI, we generated a transgenic mouse line where Grem2 is postnatally overexpressed in adult cardiomyocytes under the control of regulatory elements from the *alpha-myosin heavy chain* (α*MHC* or *Myh 6*) promoter that are active in the adult heart (TG^{Grem2}; Figure 4A; see also Methods). TG^{Grem2} mice do not exhibit differences in cardiac morphology and function as compared to *WT* counterparts (Online Table II; Online Figure VII).

TG^{Grem2} and *WT* siblings underwent permanent LAD ligation and whole heart RNA was isolated at day 0, 2 and 7 after MI. qPCR analysis showed that gain-of-Grem2-function reduced the induction levels of inflammatory gene markers such as *E-selectin* and *Vcam1* after MI with no major changes in the induction of pro-inflammatory cytokines (Figure 4B and Online Figure IIIB). Flow cytometry of cardiac cells 5 days after MI, excluding cardiomyocytes, confirmed that reduced expression of pro-inflammatory markers leads to a significant decrease in the number of $CD45^+$, $Ly6C^+$ (intermediate and high expression levels), and $F4/80^+$ cells within cardiac tissue (Figure 4C). Attenuation of inflammation correlatess with reduced induction of genes encoding the anti-inflammatory *Il-10* cytokine and *Tgfβ1* (Figure 4D). These data indicate Grem2 overexpression reduces the magnitude of the inflammatory response after MI.

Grem2 promotes functional recovery after MI

The phenotypic analysis of $Grem2^{-/-}$ and TG^{Grem2} mice indicates that Grem2 levels are inversely related to the magnitude of inflammation after MI. Excessive inflammation has been linked to poor prognosis after MI both in animal models and human patients.[43–45] To determine the effects of Grem2 gain- and loss-of-function on cardiac recovery, we compared cardiac functional parameters among *WT* controls, TG^{Grem2} and $Grem2^{-/-}$ mice by M-mode echocardiography at various time points after MI (Figure 5; Online Figure VIII).

Our data show that TG^{Grem2} and $Grem2^{-/-}$ mice have comparable ventricular dimensions and functional values to the corresponding *WT* control mice at baseline. After LAD ligation, TG^{Grem2} mice have better preserved cardiac function compared to *WT* littermate controls of C57BL/6 background, as evidenced by higher fractional shortening (FS) and ejection fraction (EF) values 21 days after MI (Figure 5A). In contrast, $Grem2^{-/-}$ mice have worse cardiac function compared to their corresponding *WT* siblings of mixed C57BL/6 and 129/Sv background (WT^{mix}).

Functional recovery in TG^{Grem2} mice was due to preservation of both systolic and diastolic dimensions with lower overall values compared to *WT* control mice at day 21 after MI (Figure 5B). Conversely, only systolic diameters are higher in $Grem2^{-/-}$ mice compared to WT^{mix} controls. These results are consistent with the $Grem2^{-/-}$ mice defects, since both the magnitude and spread of inflammation have been linked to systolic dysfunction (Figure 5B).[4] In brief, echocardiography data indicate Grem2 levels directly correlate with functional recovery after acute MI.

Grem2 regulates canonical BMP signaling in cardiomyocytes next to ischemic areas

Grem2 is known to inhibit the canonical BMP signaling pathway by preventing BMP ligand-mediated phosphorylation of Smad1/5/8.[35] To test whether Grem2 regulates canonical BMP signaling in the heart, we analyzed cardiac tissue sections from *WT*, *Grem2*$^{-/-}$ and *TG*^{Grem2} mice at day 7 after MI, shortly after the peak of *Grem2* expression. IF staining with antibodies recognizing the phosphorylated, i.e., the active form of Smad1/5/8, showed that canonical BMP signaling is active in peri-infarct cardiomyocytes of *WT* mice, in agreement with previous reports showing that BMP ligands are expressed in this region (Figure 6A).[17] The intensity of p-Smad1/5/8 was increased in *Grem2*$^{-/-}$ mice and decreased in *TG*^{Grem2} hearts as compared to *WT*s (Figure 6A,B). However, unlike the early stages after MI (Figure 1), we did not detect p-Smad1/5/8 in endothelial cells.

The p-Smad changes overlap with the Grem2 expression domain (Figure 2B) in peri-infarct area cardiomyocytes, suggesting Grem2 acts as a barrier to limit the infiltration of inflammatory cells into neighboring, relatively healthy cardiac tissue. In agreement with this notion, we observed inflammatory cells in the peri-infarct tissue past the infarct border zone in *Grem2*$^{-/-}$ hearts, whereas inflammatory cells were confined within the infarct area in *WT* controls (Figure 6C).

To test whether the increased inflammatory cell infiltration is due to p-Smad1/5/8 mediated signaling, we injected *Grem2*$^{-/-}$ mice with the canonical BMP signaling chemical inhibitor DMH1[46] and vehicle control (DMSO) on day 2, 3, and 4 after MI, which correspond to the peak days of inflammation. We used DMH1 because is highly specific to canonical BMP signaling without known off-target effects, as tested in various mouse disease models.[46–48] We found that DMH1 treatment rescues the pro-inflammatory phenotype in *Grem2*$^{-/-}$ mice. Flow cytometry analysis at day 5 after MI showed that treated *Grem2*$^{-/-}$ hearts have a dramatic decrease in infiltrated CD45^{+}, Ly6C^{+} and F4/80^{+} cells as compared to vehicle injected controls (Figure 6D).

Taken together, our data indicate Grem2 generates a molecular barrier at the border zone between infarcted and unaffected tissue that contains both the number and spatial extent of infiltrating inflammatory cells. In the absence of Grem2, increased p-Smad-mediated BMP signaling is responsible for excessive inflammation since canonical BMP inhibition rescues the loss-of-Grem2-phenotype.

Grem2 inhibits the pro-inflammatory effect of Bmp2 on endothelial cells

The data described above suggest that secretion of Grem2 protein by peri-infarct cardiomyocytes regulates the extent of inflammation by affecting directly or indirectly the pro-inflammatory phenotype of cardiac endothelial cells. Further gene expression analysis at various time points after MI showed that *Tnfα* is induced first, followed by *Bmp2* and then *Grem2* (Figure 7A). To investigate whether the sequential temporal induction patterns of the three genes after MI are linked, we tested the effects of TNFα, BMP2 and Grem2 on the human microvascular endothelial cell line HMEC-1. We found that TNFα induces expression of *E-SELECTIN,* as expected, however it also induces *BMP2*, suggesting TNFα contributes to the induction of the *Bmp2* gene after MI (Figure 7B). BMP2 in turn induces

E-SELECTIN expression in endothelial cells (Figure 7C). BMP2 also stimulates *GREM2* expression, suggesting BMP2 induces a negative regulatory loop to limit its own activity (Figure 7D).

To determine whether: a) BMP2 acts synergistically with TNFα and, b) Grem2 blocks the pro-inflammatory effect of BMP2 on endothelial cells, we treated HMEC-1 with TNFα, BMP2 and Grem2 in different combinations (Figure 7E,F). When protein factors are added alone, both TNFα and BMP2 induce *E-SELECTIN* expression. Co-stimulation with TNFα and BMP2 leads to *E-SELECTIN* induction levels higher than either factor alone, suggesting TNFα and BMP2 have a synergistic or additive effect. Grem2 does not affect the TNFα induction of *E-SELECTIN*, but completely inhibits the BMP2 effect. In similar fashion, co-incubation with TNFα, BMP2 and Grem2 reduces *E-SELECTIN* levels to those induced by TNFα treatment alone (Figure 7E). In accordance with its function as a canonical BMP signaling antagonist, Grem2 blocks induction of BMP signaling target *ID2*, whereas TNFα alone has no effect on *ID2* expression, although it reduces the fold induction of *ID2* by BMP2 (Online Figure IX). Treating cells with the chemical inhibitor of canonical BMP signaling DMH1 showed similar effects as Grem2, indicating that BMP2-stimulated induction of *E-SELECTIN* is due to activation of canonical BMP signaling (Figure 7F).

To test the functional significance of the modulation of pro-inflammatory gene expression in endothelial cells by Grem2, we performed cell adhesion assays of monocytes to endothelial cells *in vitro*. These assays showed that preincubation of endothelial cells with BMP2 increases adhesion of monocytes to endothelial cells and further enhances the TNFα effect. Incubation with Grem2 abolishes the BMP2 effect, but not that of TNFα (Figure 7G). In contrast, pre-incubation of monocytes with BMP2 and/or Grem2 has no effect on their adhesion to endothelial cells (Online Figure X). Moreover, immunofluorescence analysis of infarct areas with antibodies recognizing p-Smad1/5/8 and CD45 to determine canonical BMP signaling activity in infiltrating inflammatory cells shows no detectable p-Smad1/5/8 i.e., canonical BMP signaling in inflammatory cells, and this pattern does not change in the $Grem2^{-/-}$ mice (Online Figure XI). These data further support the idea that the primary cellular targets of Grem2 are the endothelial cells.

Together, our data suggest a sequential relationship among MI-induced Tnfα, Bmp2 and Grem2, where Tnfα induces Bmp2 and Bmp2 synergizes with Tnfα to further increase the pro-inflammatory phenotype of endothelial cells. Grem2 induction then inhibits canonical BMP signaling and the positive effect of Bmp2 on inflammatory gene expression.

Systemic Grem2 administration attenuates inflammation after MI

The results obtained in TG^{Grem2} mice and isolated endothelial cells suggest that Grem2 is sufficient to attenuate cardiac tissue inflammation after ischemic injury. To test whether this activity is confined to a specific time window after MI and does not depend on structural or functional changes caused by permanent Grem2 overexpression in the heart of TG^{Grem2} mice, we injected *WT* mice intraperitoneally with Grem2 protein at day 2, 3, and 4 after MI, during the critical time window of the inflammatory phase, isolated hearts at day 5 after MI, prepared single cell suspensions of non-cardiomyocyte cells and performed flow cytometry using antibodies recognizing specific immune cell types. As shown in Figure 8A, there is a

significant decrease in the immune cell infiltrate, namely $CD45^+$, $Ly6C^+$ and $F4/80^+$ cells, in the hearts of Grem2-injected mice as compared to saline-injected controls. These results demonstrate that the anti-inflammatory phenotype in TG^{Grem2} after MI can be recapitulated by systemic administration of Grem2 protein during the inflammation phase of cardiac tissue repair.

In conclusion, our data support the following model of cardiac tissue repair: induction of pro-inflammatory cytokines such as Tnfα after MI initiates a transient inflammatory response, which is sustained by subsequent induction of Bmp2 by Tnfα. Bmp2 increases the magnitude of inflammation through induction of pro-inflammatory cell adhesion membrane proteins in endothelial cells. Grem2 is then induced as part of a negative feedback loop to inhibit Bmp2's pro-inflammatory activity and act as a barrier of inflammation at the infarct border zone (Figure 8B).

DISCUSSION

Here we provide evidence for a new mechanism that regulates the magnitude and extent of the inflammatory response after myocardial infarction. Specifically, we show that the BMP antagonist Grem2 is robustly and transiently induced after myocardial infarction during the late inflammatory phase and the early proliferative phase of granulation tissue formation. Genetic loss and gain of function approaches revealed that Grem2 a) controls the magnitude of the inflammatory cell infiltration, although not its long-term duration and, b) acts as a molecular barrier to limit infiltration of inflammatory cells in the relatively healthy cardiac tissue adjacent to the infarct border zone. Grem2 administration during the inflammatory phase of cardiac tissue repair after MI decreases the number of inflammatory cells recruited to the infarct site. Our results further demonstrate that the anti-inflammatory effects of Grem2 depend, at least in part, on suppression of canonical BMP signaling through inhibition of Smad1/5/8 phosphorylation within ventricular tissue at the infarct border zone. In agreement with this idea, administration of DMH1, a chemical inhibitor of canonical BMP signaling, rescued the inflammatory phenotype in $Grem2^{-/-}$ mice. The effects of Grem2 in attenuating the inflammatory response correlate with a significant amelioration of ventricular function after MI, as evidenced by improved systolic and diastolic parameters in the TG^{Grem2} mice that overexpress Grem2 in cardiomyocytes. In contrast, cardiac function after MI further deteriorated over time in $Grem2^{-/-}$ mice as compared to *WT* controls.

Grem2 appears to be an integral part of an orchestrated sequence of events that regulates the inflammatory response. Our results suggest that this sequence starts with induction of Bmp2 by Tnfα, which is released shortly after cardiac tissue injury. Bmp2 then acts synergistically or additively with Tnfα to further increase and sustain the induction of pro-inflammatory membrane proteins in endothelial cells, as the Tnfα effects decrease. The pro-inflammatory action of Bmp2 is then blocked by Grem2, which itself is induced by Bmp2, thus forming a negative regulatory loop. This concept is supported by the sequential induction of *Tnfα*, *Bmp2* and *Grem2* after MI, each approximately 24 hours apart. *In vitro* assays showing Bmp2 acts on endothelial cells to promote cell adhesion of monocytes, the consistent changes in the number of inflammatory cells across a wide spectrum of various immune cell types, and histological analyses showing minimal changes in BMP signaling in infiltrating

leukocytes, all suggest that the main cellular target of Grem2 in the regulation of the inflammatory response in the heart are the endothelial cells. However, at present we cannot exclude that Grem2 may also affect inflammatory cell differentiation, activation or mobilization prior to their recruitment in the infarct area.

Previous studies have linked BMP ligands to stimulation of the pro-inflammatory phenotype of endothelial cells and adhesion of leukocytes in response to shear stress *in vitro*.[49–52] Likewise, BMP signaling has been associated with promotion of inflammation in models of atherosclerosis and with anemia caused by chronic inflammatory conditions.[51,53,54] Conversely, BMP antagonists such as BMPER and Noggin can inhibit inflammation by reducing the expression of pro-inflammatory cell adhesion molecules,[51,53,55] and administration of chemical inhibitors of BMP signaling such as LDN-193189 and dorsomorphin reduced vascular inflammation and atherosclerosis.[52,56,57] Our data indicate that BMP signaling also plays an important role in the cardiac repair process after MI. Although it was known that BMP ligands might cause cardiomyocyte apoptosis, to our knowledge, ours is the first study to show that canonical BMP signaling activation after MI controls the magnitude of the inflammatory response. Importantly, this is the first indication that induction of the BMP antagonist Grem2 in the heart after MI may be a critical mechanism in the suppression of the vascular pro-inflammatory phenotype, as a way to reduce and eventually stop recruitment of circulating leukocytes.

Grem2 protein is synthesized primarily in peri-infarct cardiomyocytes, a domain that overlaps both with the expression of BMP2 after MI and the area of p-Smad1/5/8, i.e., canonical BMP signaling activation. Histological analysis in *Grem2*$^{-/-}$ mice suggests that Grem2 inhibits p-Smad activation. Some p-Smad1/5/8 persists in cardiomyocytes, even with Grem2 induction, which may be due to the presence of ligands such as GDFs or Activins that can induce Smad1/5/8 phosphorylation, but are not inhibited by Grem2.[26] Persistent activity suggests that additional canonical BMP signaling inhibition may be required after MI to supplement Grem2. Previous reports have linked activation of BMP signaling to cardiomyocyte apoptosis[15] during the early stages of ischemia/reperfusion injury, as well as fibrosis and hypertrophy[48], so Grem2 may have additional cardioprotective properties.

We have previously shown that Grem2 is necessary for cardiac asymmetry and atrial development in zebrafish. However, it appears that Grem2 is dispensable for mouse development. This result is not without precedent among BMP signaling components. For example, single Bmp5, Bmp6, and Bmp7 knockout mice are viable, but double knockouts of either Bmp5/7 or Bmp6/7 are embryonic lethal due to cardiac developmental defects.[58–61] It is likely that, as with Bmp ligands, there is redundancy among BMP antagonists in cardiac development. Such redundancy may also happen in the adult heart. Although Grem2 is the BMP antagonist induced the highest after MI, the heart maintains expression of a number of BMP antagonists such as *Chordin, Sost*, *Twsg1* and *Dan*. There are also low levels of *Noggin* expression. Sost does not inhibit Bmp2 and thus it is unlikely Sost plays a role in the inflammatory response, which is dominated by Bmp2 induction. Dan, Chordin, and Twsg1 are weaker antagonists than Grem2 and may not compensate for Grem2 in the peri-infarct area, where Grem2 is prominently induced.[36,37] It will be informative to generate double loss-of-function model by crossing the *Grem2*$^{-/-}$ mice to mice with conditional inactivation

of other BMP antagonists to directly test redundant functions during development or after injury.

Increased numbers of infiltrating immune cells, or prolonged inflammation negatively impacts subsequent steps of cardiac repair and functional recovery.[4] Activated immune cells may continue to degrade matrix, impede angiogenesis, or affect myofibroblast proliferation and differentiation. However, clinical trials testing whether blocking inflammation improves outcomes have so far produced mixed results. For example, inhibitors of the complement system, TNFα, or integrins required for immune cell binding showed no significant improvement of infarct size and MI outcomes.[45,62–65] Glucocorticoids actually had severe adverse effects, likely due to their interference with functions that are essential for healing.[66] On the other hand, inhibitors of activated T-cells such as cyclosporine[67] and the P-selectin antagonist inclacumab,[68] did show promising results, indicating that moderating inflammation can be beneficial for cardiac repair after MI. However, the benefits of cyclosporine use after MI could not be replicated in a larger clinical trial.[69] The failure or modest success to reduce infarct size in MI patients by targeting direct players of reparative inflammatory processes underscores the need to better understand the endogenous regulatory mechanisms that control the temporal and spatial extent of inflammation. Even if blocking overactive post-infarction inflammation does not affect the size of the infarct, it might moderate dilative remodeling.

Recent crystallographic evidence revealed that Grem2 folds into a unique tertiary shape that has not been described before. Specifically, Grem2 dimerizes in a head-to-tail manner, unlike the head-to-head pairing of Noggin.[20,70] This head-to-tail arrangement gives rise to a concave and convex 3-D structure, which precludes Grem2 from wrapping around BMP dimers as Noggin does.[20,23,70] We currently test whether this unique structural arrangement is also critical for the function of Grem2 in cardiac repair. Future biochemical analyses may identify critical structural motifs, which could be exploited to design molecules that mimic the biological effects of Grem2. Recognizing these mechanisms may offer novel insights in the cardiac healing process and provide new ways to regulate inflammation in a physiological manner. Moreover, due to the wide interest in regulating BMP signaling in bone fractures, osteoporosis and cancer, a number of chemical compounds and peptides, to either promote or hinder BMP signaling, are being developed for clinical use.[71,72] Our findings may facilitate future repurposing of these new pharmacological resources for potential treatment of MI patients to expand current strategies that aim to restore circulation to infarcted areas with thrombolytics and percutaneous interventions.

Supplementary Material

Refer to Web version on PubMed Central for supplementary material.

Acknowledgments

We thank members of the Cardiovascular Pathophysiology and Complications Core, the Cell Imaging Shared Resource, the Translational Pathology Shared Resource, the Transgenic Mouse/ES Cell Resource, and the Molecular Cell Biology Resource at Vanderbilt University Medical Center for technical assistance. This work also utilized the cores of the Vanderbilt Diabetes Research and Training Center funded by grant 020593 from the National Institute of Diabetes and Digestive and Kidney Disease. We thank Jennifer Skelton for supervising the

gene targeting and mouse blastocyst microinjection procedures; Lianli Ma, Lin Zhong, and Zhizhang Wang for performing mouse surgeries and echocardiograms; Vineeta Tanwar for help with the initial mouse colony maintenance; Daniel Levic and Ela W. Knapik for help with histological analyses; and David T. Paik for providing heart samples for histological analysis.

SOURCES OF FUNDING

This work was supported by National Institutes of Health grants HL083958 and HL100398 to AKH, GM114640 to TBT and AKH; Institutional Support from Vanderbilt University Medical Center to AKH; and, a T32 Program in Cardiovascular Mechanisms: Training in Investigation (HL007411) fellowship to LNS.

Nonstandard Abbreviations and Acronyms

BMP	Bone Morphogenetic Protein
EF	Ejection Fraction
FS	Fractional Shortening
Grem2	Gremlin 2
HF	Heart Failure
Icam1	Intercellular cell adhesion molecule 1
IF	Immunofluorescence
ID	Inhibitor of Differentiation, or Inhibitor of DNA binding
LV	Left Ventricle
LVIDd	Left Ventricular Internal Dimension, dystolic
LVIDs	Left Ventricular Internal Dimension, systolic
αMHC	Alpha-Myosin Heavy Chain (Myh6)
MI	Myocardial Infarction
αSMA	Alpha Smooth Muscle Actin
TGFβ	Transforming Growth Factor β
TNFα	Tumor Necrotic Factor alpha
Vcam1	Vascular cell adhesion molecule 1
WT	Wild-type

References

1. Mozaffarian D, et al. Heart Disease and Stroke Statistics-2016 Update: A report from the American Heart Association. Circulation. 2016; 133:e38–e360. [PubMed: 26673558]
2. McMurray JJV. Clinical practice. Systolic heart failure. N Engl J Med. 2010; 362:228–238. [PubMed: 20089973]
3. Konstantinidis K, Whelan RS, Kitsis RN. Mechanisms of cell death in heart disease. Arterioscler Thromb Vasc Biol. 2012; 32:1552–1562. [PubMed: 22596221]

4. Frangogiannis NG. The inflammatory response in myocardial injury, repair, and remodelling. Nat Rev Cardiol. 2014; 11:255–265. [PubMed: 24663091]
5. Boudoulas KD, Hatzopoulos AK. Cardiac repair and regeneration: the Rubik's cube of cell therapy for heart disease. Dis Model Mech. 2009; 2:344–358. [PubMed: 19553696]
6. Virag JI, Murry CE. Myofibroblast and endothelial cell proliferation during murine myocardial infarct repair. Am J Pathol. 2003; 163:2433–2440. [PubMed: 14633615]
7. Aisagbonhi O, Rai M, Ryzhov S, Atria N, Feoktistov I, Hatzopoulos AK. Experimental myocardial infarction triggers canonical Wnt signaling and endothelial-to-mesenchymal transition. Dis Model Mech. 2011; 4:469–483. [PubMed: 21324930]
8. Paik DT, Rai M, Ryzhov S, Sanders LN, Aisagbonhi O, Funke MJ, Feoktistov I, Hatzopoulos AK. Wnt10b gain-of-function improves cardiac repair by arteriole formation and attenuation of fibrosis. Circ Res. 2015; 117:804–816. [PubMed: 26338900]
9. van Wijk B, Moorman AFM, van den Hoff MJB. Role of bone morphogenetic proteins in cardiac differentiation. Cardiovasc Res. 2007; 74:244–255. [PubMed: 17187766]
10. Kruithof BPT, van Wijk B, Somi S, Kruithof-de Julio M, Pérez Pomares JM, Weesie F, Wessels A, Moorman AFM, van den Hoff MJB. BMP and FGF regulate the differentiation of multipotential pericardial mesoderm into the myocardial or epicardial lineage. Dev Biol. 2006; 295:507–522. [PubMed: 16753139]
11. Breckenridge RA, Mohun TJ, Amaya E. A role for BMP signalling in heart looping morphogenesis in Xenopus. Dev Biol. 2001; 232:191–203. [PubMed: 11254357]
12. Marques SR, Yelon D. Differential requirement for BMP signaling in atrial and ventricular lineages establishes cardiac chamber proportionality. Dev Biol. 2009; 328:472–482. [PubMed: 19232521]
13. de Pater E, Ciampricotti M, Priller F, Veerkamp J, Strate I, Smith K, Lagendijk AK, Schilling TF, Herzog W, Abdelilah-Seyfried S, Hammerschmidt M, Bakkers J. Bmp signaling exerts opposite effects on cardiac differentiation. Circ Res. 2012; 110:578–587. [PubMed: 22247485]
14. Ma L, Lu M-F, Schwartz RJ, Martin JF. Bmp2 is essential for cardiac cushion epithelial-mesenchymal transition and myocardial patterning. Development. 2005; 132:5601–5611. [PubMed: 16314491]
15. Pachori AS, Custer L, Hansen D, Clapp S, Kemppa E, Klingensmith J. Bone morphogenetic protein 4 mediates myocardial ischemic injury through JNK-dependent signaling pathway. J Mol Cell Cardiol. 2010; 48:1255–1265. [PubMed: 20096288]
16. Wu X, Sagave J, Rutkovskiy A, Haugen F, Baysa A, Nygård S, Czibik G, Dahl CP, Gullestad L, Vaage J, Valen G. Expression of bone morphogenetic protein 4 and its receptors in the remodeling heart. Life Sci. 2014; 97:145–154. [PubMed: 24398041]
17. Chang S-A, Lee EJ, Kang H-J, Zhang S-Y, Kim J-H, Li L, Youn S-W, Lee C-S, Kim K-H, Won J-Y, Sohn J-W, Park K-W, Cho H-J, Yang S-E, Oh WI, Yang YS, Ho W-K, Park Y-B, Kim H-S. Impact of myocardial infarct proteins and oscillating pressure on the differentiation of mesenchymal stem cells: effect of acute myocardial infarction on stem cell differentiation. Stem Cells. 2008; 26:1901–1912. [PubMed: 18403756]
18. Yadin D, Knaus P, Mueller TD. Structural insights into BMP receptors: Specificity, activation and inhibition. Cytokine Growth Factor Rev. 2016; 27:13–34. [PubMed: 26690041]
19. Umulis D, O'Connor MB, Blair SS. The extracellular regulation of bone morphogenetic protein signaling. Development. 2009; 136:3715–3728. [PubMed: 19855014]
20. Groppe J, Greenwald J, Wiater E, Rodriguez-Leon J, Economides AN, Kwiatkowski W, Affolter M, Vale WW, Izpisua Belmonte JC, Choe S. Structural basis of BMP signalling inhibition by the cystine knot protein Noggin. Nature. 2002; 420:636–642. [PubMed: 12478285]
21. Pearce JJ, Penny G, Rossant J. A mouse cerberus/Dan-related gene family. Dev Biol. 1999; 209:98–110. [PubMed: 10208746]
22. Avsian-Kretchmer O, Hsueh AJW. Comparative genomic analysis of the eight-membered ring cystine knot-containing bone morphogenetic protein antagonists. Mol Endocrinol. 2004; 18:1–12. [PubMed: 14525956]
23. Nolan K, Thompson TB. The DAN family: modulators of TGF-β signaling and beyond. Protein Sci. 2014; 23:999–1012. [PubMed: 24810382]

24. Minabe-Saegusa C, Saegusa H, Tsukahara M, Noguchi S. Sequence and expression of a novel mouse gene PRDC (protein related to DAN and cerberus) identified by a gene trap approach. Dev Growth Differ. 1998; 40:343–353. [PubMed: 9639362]
25. Lu MM, Yang H, Zhang L, Shu W, Blair DG, Morrisey EE. The bone morphogenic protein antagonist gremlin regulates proximal-distal patterning of the lung. Dev Dyn. 2001; 222:667–680. [PubMed: 11748835]
26. Sudo S, Avsian-Kretchmer O, Wang LS, Hsueh AJW. Protein related to DAN and cerberus is a bone morphogenetic protein antagonist that participates in ovarian paracrine regulation. J Biol Chem. 2004; 279:23134–23141. [PubMed: 15039429]
27. Kriebitz NN, Kiecker C, McCormick L, Lumsden A, Graham A, Bell E. PRDC regulates placode neurogenesis in chick by modulating BMP signalling. Dev Biol. 2009; 336:280–292. [PubMed: 19836367]
28. Ideno H, Takanabe R, Shimada A, Imaizumi K, Araki R, Abe M, Nifuji A. Protein related to DAN and cerberus (PRDC) inhibits osteoblastic differentiation and its suppression promotes osteogenesis in vitro. Exp Cell Res. 2009; 315:474–484. [PubMed: 19073177]
29. Cahill E, Costello CM, Rowan SC, Harkin S, Howell K, Leonard MO, Southwood M, Cummins EP, Fitzpatrick SF, Taylor CT, Morrell NW, Martin F, McLoughlin P. Gremlin plays a key role in the pathogenesis of pulmonary hypertension. Circulation. 2012; 125:920–930. [PubMed: 22247494]
30. Gao H, Chakraborty G, Lee-Lim AP, Mo Q, Decker M, Vonica A, Shen R, Brogi E, Brivanlou AH, Giancotti FG. The BMP inhibitor Coco reactivates breast cancer cells at lung metastatic sites. Cell. 2012; 150:764–779. [PubMed: 22901808]
31. Koli K, Myllärniemi M, Vuorinen K, Salmenkivi K, Ryynänen MJ, Kinnula VL, Keski-Oja J. Bone morphogenetic protein-4 inhibitor gremlin is overexpressed in idiopathic pulmonary fibrosis. Am J Pathol. 2006; 169:61–71. [PubMed: 16816361]
32. Dolan V, Murphy M, Sadlier D, Lappin D, Doran P, Godson C, Martin F, O'Meara Y, Schmid H, Henger A, Kretzler M, Droguett A, Mezzano S, Brady HR. Expression of gremlin, a bone morphogenetic protein antagonist, in human diabetic nephropathy. Am J Kidney Dis. 2005; 45:1034–1039. [PubMed: 15957132]
33. Müller II, Knapik EW, Hatzopoulos AK. Expression of the protein related to Dan and Cerberus gene--prdc--During eye, pharyngeal arch, somite, and swim bladder development in zebrafish. Dev Dyn. 2006; 235:2881–2888. [PubMed: 16921498]
34. Muller II, Melville DB, Tanwar V, Rybski WM, Mukherjee A, Shoemaker MB, Wang W-D, Schoenhard JA, Roden DM, Darbar D, Knapik EW, Hatzopoulos AK. Functional modeling in zebrafish demonstrates that the atrial-fibrillation-associated gene GREM2 regulates cardiac laterality, cardiomyocyte differentiation and atrial rhythm. Dis Model Mech. 2013; 6:332–341. [PubMed: 23223679]
35. Tanwar V, Bylund JB, Hu J, Yan J, Walthall JM, Mukherjee A, Heaton WH, Wang W-D, Potet F, Rai M, Kupershmidt S, Knapik EW, Hatzopoulos AK. Gremlin 2 promotes differentiation of embryonic stem cells to atrial fate by activation of the JNK signaling pathway. Stem Cells. 2014; 32:1774–1788. [PubMed: 24648383]
36. Nolan K, Kattamuri C, Luedeke DM, Angerman EB, Rankin SA, Stevens ML, Zorn AM, Thompson TB. Structure of neuroblastoma suppressor of tumorigenicity 1 (NBL1): insights for the functional variability across bone morphogenetic protein (BMP) antagonists. J Biol Chem. 2015; 290:4759–4771. [PubMed: 25561725]
37. Zhang J-L, Huang Y, Qiu L-Y, Nickel J, Sebald W. von Willebrand factor type C domain-containing proteins regulate bone morphogenetic protein signaling through different recognition mechanisms. J Biol Chem. 2007; 282:20002–20014. [PubMed: 17483092]
38. Nahrendorf M, Swirski FK, Aikawa E, Stangenberg L, Wurdinger T, Figueiredo J-L, Libby P, Weissleder R, Pittet MJ. The healing myocardium sequentially mobilizes two monocyte subsets with divergent and complementary functions. J Exp Med. 2007; 204:3037–3047. [PubMed: 18025128]
39. Yan X, Anzai A, Katsumata Y, Matsuhashi T, Ito K, Endo J, Yamamoto T, Takeshima A, Shinmura K, Shen W, Fukuda K, Sano M. Temporal dynamics of cardiac immune cell accumulation following acute myocardial infarction. J Mol Cell Cardiol. 2013; 62:24–35. [PubMed: 23644221]

40. Hulsmans M, Sam F, Nahrendorf M. Monocyte and macrophage contributions to cardiac remodeling. J Mol Cell Cardiol. 2016; 93:149–155. [PubMed: 26593722]
41. Swirski FK, Nahrendorf M, Etzrodt M, Wildgruber M, Cortez-Retamozo V, Panizzi P, Figueiredo J-L, Kohler RH, Chudnovskiy A, Waterman P, Aikawa E, Mempel TR, Libby P, Weissleder R, Pittet MJ. Identification of splenic reservoir monocytes and their deployment to inflammatory sites. Science. 2009; 325:612–616. [PubMed: 19644120]
42. Chia S, Nagurney JT, Brown DFM, Raffel OC, Bamberg F, Senatore F, Wackers FJT, Jang I-K. Association of leukocyte and neutrophil counts with infarct size, left ventricular function and outcomes after percutaneous coronary intervention for ST-elevation myocardial infarction. Am J Cardiol. 2009; 103:333–337. [PubMed: 19166685]
43. Lefer DJ, Shandelya SM, Serrano CV, Becker LC, Kuppusamy P, Zweier JL. Cardioprotective actions of a monoclonal antibody against CD-18 in myocardial ischemia-reperfusion injury. Circulation. 1993; 88:1779–1787. [PubMed: 8104739]
44. Simpson PJ, Todd RF, Fantone JC, Mickelson JK, Griffin JD, Lucchesi BR. Reduction of experimental canine myocardial reperfusion injury by a monoclonal antibody (anti-Mo1, anti-CD11b) that inhibits leukocyte adhesion. J Clin Invest. 1988; 81:624–629. [PubMed: 3339135]
45. de Lemos JA, Morrow DA, Blazing MA, Jarolim P, Wiviott SD, Sabatine MS, Califf RM, Braunwald E. Serial measurement of monocyte chemoattractant protein-1 after acute coronary syndromes: results from the A to Z trial. J Am Coll Cardiol. 2007; 50:2117–2124. [PubMed: 18036447]
46. Ao A, Hao J, Hopkins CR, Hong CC. DMH1, a novel BMP small molecule inhibitor, increases cardiomyocyte progenitors and promotes cardiac differentiation in mouse embryonic stem cells. PloS One. 2012; 7:e41627. [PubMed: 22848549]
47. Hao J, Lee R, Chang A, Fan J, Labib C, Parsa C, Orlando R, Andresen B, Huang Y. DMH1, a small molecule inhibitor of BMP type I receptors, suppresses growth and invasion of lung cancer. PloS One. 2014; 9:e90748. [PubMed: 24603907]
48. Sun B, Huo R, Sheng Y, Li Y, Xie X, Chen C, Liu H-B, Li N, Li C-B, Guo W-T, Zhu J-X, Yang B-F, Dong D-L. Bone morphogenetic protein-4 mediates cardiac hypertrophy, apoptosis, and fibrosis in experimentally pathological cardiac hypertrophy. Hypertension. 2013; 61:352–360. [PubMed: 23248151]
49. Sorescu GP, Sykes M, Weiss D, Platt MO, Saha A, Hwang J, Boyd N, Boo YC, Vega JD, Taylor WR, Jo H. Bone morphogenic protein 4 produced in endothelial cells by oscillatory shear stress stimulates an inflammatory response. J Biol Chem. 2003; 278:31128–31135. [PubMed: 12766166]
50. Csiszar A, Smith KE, Koller A, Kaley G, Edwards JG, Ungvari Z. Regulation of bone morphogenetic protein-2 expression in endothelial cells: role of nuclear factor-kappaB activation by tumor necrosis factor-alpha, H2O2, and high intravascular pressure. Circulation. 2005; 111:2364–2372. [PubMed: 15851600]
51. Sucosky P, Balachandran K, Elhammali A, Jo H, Yoganathan AP. Altered shear stress stimulates upregulation of endothelial VCAM-1 and ICAM-1 in a BMP-4- and TGF-beta1-dependent pathway. Arterioscler Thromb Vasc Biol. 2009; 29:254–260. [PubMed: 19023092]
52. Helbing T, Rothweiler R, Ketterer E, Goetz L, Heinke J, Grundmann S, Duerschmied D, Patterson C, Bode C, Moser M. BMP activity controlled by BMPER regulates the proinflammatory phenotype of endothelium. Blood. 2011; 118:5040–5049. [PubMed: 21900199]
53. Pi X, Lockyer P, Dyer LA, Schisler JC, Russell B, Carey S, Sweet DT, Chen Z, Tzima E, Willis MS, Homeister JW, Moser M, Patterson C. Bmper inhibits endothelial expression of inflammatory adhesion molecules and protects against atherosclerosis. Arterioscler Thromb Vasc Biol. 2012; 32:2214–2222. [PubMed: 22772758]
54. Steinbicker AU, Sachidanandan C, Vonner AJ, Yusuf RZ, Deng DY, Lai CS, Rauwerdink KM, Winn JC, Saez B, Cook CM, Szekely BA, Roy CN, Seehra JS, Cuny GD, Scadden DT, Peterson RT, Bloch KD, Yu PB. Inhibition of bone morphogenetic protein signaling attenuates anemia associated with inflammation. Blood. 2011; 117:4915–4923. [PubMed: 21393479]
55. Koga M, Engberding N, Dikalova AE, Chang KH, Seidel-Rogol B, Long JS, Lassègue B, Jo H, Griendling KK. The bone morphogenic protein inhibitor, noggin, reduces glycemia and vascular inflammation in db/db mice. Am J Physiol Heart Circ Physiol. 2013; 305:H747–755. [PubMed: 23812391]

56. Morrell NW, Bloch DB, Ten Dijke P, Goumans M-JTH, Hata A, Smith J, Yu PB, Bloch KD. Targeting BMP signalling in cardiovascular disease and anaemia. Nat Rev Cardiol. 2016; 13:106–120. [PubMed: 26461965]
57. Derwall M, Malhotra R, Lai CS, Beppu Y, Aikawa E, Seehra JS, Zapol WM, Bloch KD, Yu PB. Inhibition of bone morphogenetic protein signaling reduces vascular calcification and atherosclerosis. Arterioscler Thromb Vasc Biol. 2012; 32:613–622. [PubMed: 22223731]
58. Dudley AT, Robertson EJ. Overlapping expression domains of bone morphogenetic protein family members potentially account for limited tissue defects in BMP7 deficient embryos. Dev Dyn. 1997; 208:349–362. [PubMed: 9056639]
59. Kim RY, Robertson EJ, Solloway MJ. Bmp6 and Bmp7 are required for cushion formation and septation in the developing mouse heart. Dev Biol. 2001; 235:449–466. [PubMed: 11437450]
60. Solloway MJ, Dudley AT, Bikoff EK, Lyons KM, Hogan BL, Robertson EJ. Mice lacking Bmp6 function. Dev Genet. 1998; 22:321–339. [PubMed: 9664685]
61. Solloway MJ, Robertson EJ. Early embryonic lethality in Bmp5; Bmp7 double mutant mice suggests functional redundancy within the 60A subgroup. Development. 1999; 126:1753–1768. [PubMed: 10079236]
62. Chung ES, Packer M, Lo KH, Fasanmade AA, Willerson JT. Anti-TNF Therapy Against Congestive Heart Failure Investigators. Randomized, double-blind, placebo-controlled, pilot trial of infliximab, a chimeric monoclonal antibody to tumor necrosis factor-alpha, in patients with moderate-to-severe heart failure: results of the anti-TNF Therapy Against Congestive Heart Failure (ATTACH) trial. Circulation. 2003; 107:3133–3140. [PubMed: 12796126]
63. Baran KW, Nguyen M, McKendall GR, Lambrew CT, Dykstra G, Palmeri ST, Gibbons RJ, Borzak S, Sobel BE, Gourlay SG, Rundle AC, Gibson CM, Barron HV. Limitation of Myocardial Infarction Following Thrombolysis in Acute Myocardial Infarction (LIMIT AMI) Study Group. Double-blind, randomized trial of an anti-CD18 antibody in conjunction with recombinant tissue plasminogen activator for acute myocardial infarction: limitation of myocardial infarction following thrombolysis in acute myocardial infarction (LIMIT AMI) study. Circulation. 2001; 104:2778–2783. [PubMed: 11733394]
64. Faxon DP, Gibbons RJ, Chronos NAF, Gurbel PA, Sheehan F. The effect of blockade of the CD11/CD18 integrin receptor on infarct size in patients with acute myocardial infarction treated with direct angioplasty: the results of the HALT-MI study. J Am Coll Cardiol. 2002; 40:1199–1204. [PubMed: 12383565]
65. Armstrong PW, Granger CB, Adams PX, Hamm C, Holmes DJ, O'Neill WW, Todaro TG, Vahanian A, Van de Werf F. Pexelizumab for acute ST-elevation myocardial infarction in patients undergoing primary percutaneous coronary intervention: a randomized controlled trial. JAMA. 2007; 297:43–51. [PubMed: 17200474]
66. Roberts R, DeMello V, Sobel BE. Deleterious effects of methylprednisolone in patients with myocardial infarction. Circulation. 1976; 53:I204–206. [PubMed: 1253361]
67. Piot C, Croisille P, Staat P, Thibault H, Rioufol G, Mewton N, Elbelghiti R, Cung TT, Bonnefoy E, Angoulvant D, Macia C, Raczka F, Sportouch C, Gahide G, Finet G, André-Fouët X, Revel D, Kirkorian G, Monassier J-P, Derumeaux G, Ovize M. Effect of cyclosporine on reperfusion injury in acute myocardial infarction. N Engl J Med. 2008; 359:473–481. [PubMed: 18669426]
68. Tardif J-C, Tanguay J-F, Wright SS, Duchatelle V, Petroni T, Grégoire JC, Ibrahim R, Heinonen TM, Robb S, Bertrand OF, Cournoyer D, Johnson D, Mann J, Guertin M-C, L'Allier PL. Effects of the P-selectin antagonist inclacumab on myocardial damage after percutaneous coronary intervention for non-ST-segment elevation myocardial infarction: results of the SELECT-ACS trial. J Am Coll Cardiol. 2013; 61:2048–2055. [PubMed: 23500230]
69. Cung T-T, Morel O, Cayla G, Rioufol G, Garcia-Dorado D, Angoulvant D, Bonnefoy-Cudraz E, Guérin P, Elbaz M, Delarche N, Coste P, Vanzetto G, Metge M, Aupetit J-F, Jouve B, Motreff P, Tron C, Labeque J-N, Steg PG, Cottin Y, Range G, Clerc J, Claeys MJ, Coussement P, Prunier F, Moulin F, Roth O, Belle L, Dubois P, Barragan P, Gilard M, Piot C, Colin P, De Poli F, Morice M-C, Ider O, Dubois-Randé J-L, Unterseeh T, Le Breton H, Béard T, Blanchard D, Grollier G, Malquarti V, Staat P, Sudre A, Elmer E, Hansson MJ, Bergerot C, Boussaha I, Jossan C, Derumeaux G, Mewton N, Ovize M. Cyclosporine before PCI in patients with acute myocardial infarction. N Engl J Med. 2015; 373:1021–1031. [PubMed: 26321103]

70. Nolan K, Kattamuri C, Luedeke DM, Deng X, Jagpal A, Zhang F, Linhardt RJ, Kenny AP, Zorn AM, Thompson TB. Structure of Protein Related to Dan and Cerberus: Insights into the mechanism of Bone Morphogenetic Protein antagonism. Structure. 2013; 21:1417–1429. [PubMed: 23850456]

71. Sanvitale CE, Kerr G, Chaikuad A, Ramel M-C, Mohedas AH, Reichert S, Wang Y, Triffitt JT, Cuny GD, Yu PB, Hill CS, Bullock AN. A new class of small molecule inhibitor of BMP signaling. PLoS ONE. 2013; 8:e62721. [PubMed: 23646137]

72. Cao Y, Wang C, Zhang X, Xing G, Lu K, Gu Y, He F, Zhang L. Selective small molecule compounds increase BMP-2 responsiveness by inhibiting Smurf1-mediated Smad1/5 degradation. Sci Rep. 2014; 4:4965. [PubMed: 24828823]

NOVELTY AND SIGNIFICANCE

What Is Known?

- Recruitment of inflammatory cells is an early critical step in the repair of heart tissue after a myocardial infarction (MI).
- Although inflammatory cells are necessary to clear debris from dead cells, excessive inflammation after MI is correlated with adverse cardiac remodeling and poor prognosis.
- Bone morphogenetic proteins (BMPs), which are critical for heart development, are induced shortly after MI, but their role in heart repair is largely unknown.

What New Information Does This Article Contribute?

- The BMP signaling inhibitor Gremlin 2 (Grem2) is a secreted protein that is transiently induced in infarct border cardiomyocytes at the end of the inflammatory phase after MI, at the site of BMP signaling activation.
- BMP signaling contributes to the induction of cell adhesion membrane proteins in endothelial cells that capture and recruit inflammatory cells after MI.
- Grem2 gene inactivation intensifies BMP signaling leading to a dramatic increase in the number of infiltrating inflammatory cells after MI and further deterioration of heart function, whereas Grem2 overexpression in the heart, or injection of Grem2 protein shortly after MI attenuates inflammation and improves recovery.

Although unregulated inflammation has been linked to adverse effects in the heart, previous anti-inflammatory treatments in MI patients have been mostly unsuccessful. The failure or modest success of clinical trials aiming to reduce infarct size in MI patients, by targeting direct players of the inflammatory processes, underscores the need to better understand the natural mechanisms that control inflammation in the injured heart tissue. In this manuscript, we provide evidence for a new mechanism that determines the magnitude and extent of the inflammatory response after MI. Specifically, our data show that Tumor Necrosis Factor alpha (TNFα) induction after MI initiates a transient inflammatory response, which is sustained by subsequent induction of the BMP ligand BMP2. BMP2 increases the magnitude of inflammation through upregulation of pro-inflammatory cell adhesion membrane proteins in endothelial cells. Grem2 is then induced by BMP2 as part of a negative feedback loop to inhibit the pro-inflammatory activity of canonical BMP signaling and act as a barrier to inflammation at the infarct border zone. Our findings suggest that BMP antagonists like Grem2 could attenuate inflammation, and thereby improve heart recovery MI.

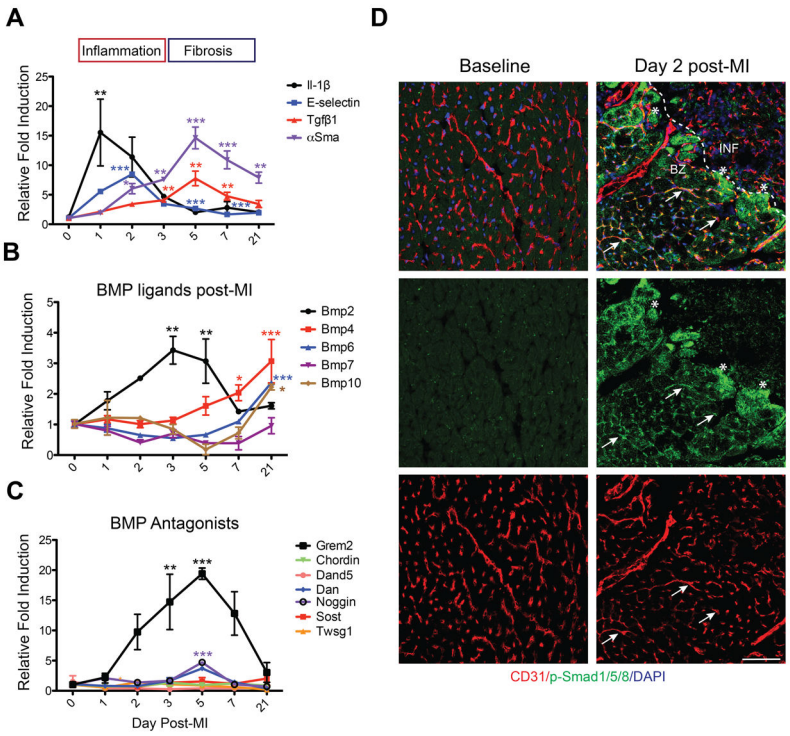

Figure 1. Dynamic changes in the expression of BMP signaling components and BMP antagonists after myocardial infarction

(A–C) Whole mouse heart RNA samples were isolated at day 0 (baseline, prior to injury), 1, 2, 3, 5, 7 and 21 post-MI and analyzed by qPCR. Values at baseline were set as 1. **(A)** Sequential induction of inflammation (*Il-10β* and *E- selectin*) and fibrosis (*Tgfβ1* and *αSma*) associated genes after MI. **(B)** Expression analysis of BMP ligands shows that *Bmp2* is transiently induced during the inflammatory phase of the post-MI repair process, followed by induction of *Bmp4, Bmp6, and Bmp10*. **(C)** Expression analysis of BMP antagonists shows *Grem2* is the main antagonist induced after MI, starting at the late inflammatory phase and peaking at day 5. ** P < 0.05; ** P < 0.01; *** P< 0.001* compared to day 0. One-way ANOVA with Dunnett's multiple comparisons test. N=3 for all time points. All data are means ± SEM. **(D)** Immunofluorescence (IF) analysis with antibodies recognizing p-Smad1/5/8 (green) and CD31 (red) shows that p-Smad1/5/8 is not present in normal cardiac tissue at baseline prior to MI, but is activated in peri-infarct area endothelial cells at day 2 post-MI (representative examples marked with arrows) and in cardiomyocytes (asterisks). DAPI (blue) marks cellular nuclei. Scale bar 50 μm. Abbreviations: BZ=border zone; INF=infarct; *Il-1β: Interleukin 1β; Tgfβ1: Transforming growth factor β1; αSma: alpha Smooth muscle actin; Grem2: Gremlin 2; Dand5: DAN domain family member 5 (also Dante, or Coco); Dan: Neuroblastoma 1 (Nbl1); Sost: Sclerostin; Twsg1: Twisted gastrulation BMP signaling modulator 1.*

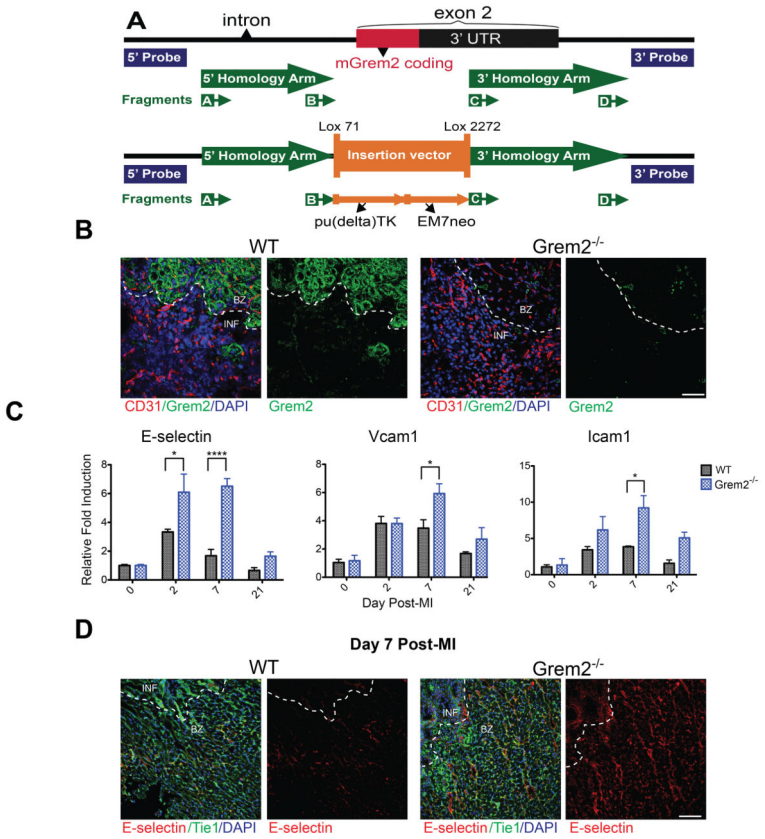

Figure 2. Loss of Grem2 increases expression of genes encoding endothelial cell membrane proteins that mediate inflammatory cell recruitment after MI

(A) Schematic diagram of the Grem2 gene knockout strategy before (upper panel) and after homologous recombination (lower panel). The entire coding region of Grem2 in exon2 was replaced by the pu(delta)TK/EM7neo selection cassette as described in the Methods. The location of fragments A–D used to modify the corresponding BAC clone, the extent of homology arms, and the position of DNA probes used for screening putative *Grem2*$^{-/-}$ ES clones are indicated. **(B)** IF analysis with antibodies recognizing Grem2 (green) and CD31 (red) shows that Grem2 protein is induced in the peri-infarct area. Grem2 expression appears primarily in cardiomyocytes, but not CD31^{+} endothelial cells. Grem2 protein expression is missing in *Grem2*$^{-/-}$ mice. DAPI marks cellular nuclei. Scale bars 100 μm. BZ=border zone, INF=infarct. **(C)** qPCR analysis of whole heart RNA samples isolated from *WT* and *Grem2*$^{-/-}$ mice at days 0, 2, 7 and 21 post-MI. Induction levels of gene encoding endothelial cell-specific adhesion membrane proteins *E-selectin*, *Vcam1* and *Icam1* are significantly higher in *Grem2*$^{-/-}$ hearts compared to WT counterparts. ** P < 0.05; **** P < 0.0001*. Two-way ANOVA with Bonferroni multiple comparisons test. N=3 for all time points. All data are means ± SEM. **(D)** IF analysis of cardiac tissue sections at day 7 post-MI shows E-selectin protein expression (red) persists in endothelial cells (Tie1, green) in the infarct (INF) and peri-infarct border zone (BZ) areas in *Grem2*$^{-/-}$ hearts compared to *WT*s. DAPI marks cellular nuclei. Scale bars 100 μm. Abbreviations: pu(Δ)TK: fusion of puromycin and truncated thymidine kinase genes; EM7neo: kanamycin resistance gene under the synthetic

bacterial EM7 promoter; *Vcam1: Vascular cell adhesion molecule 1; Icam1: Intercellular cell adhesion molecule 1.*

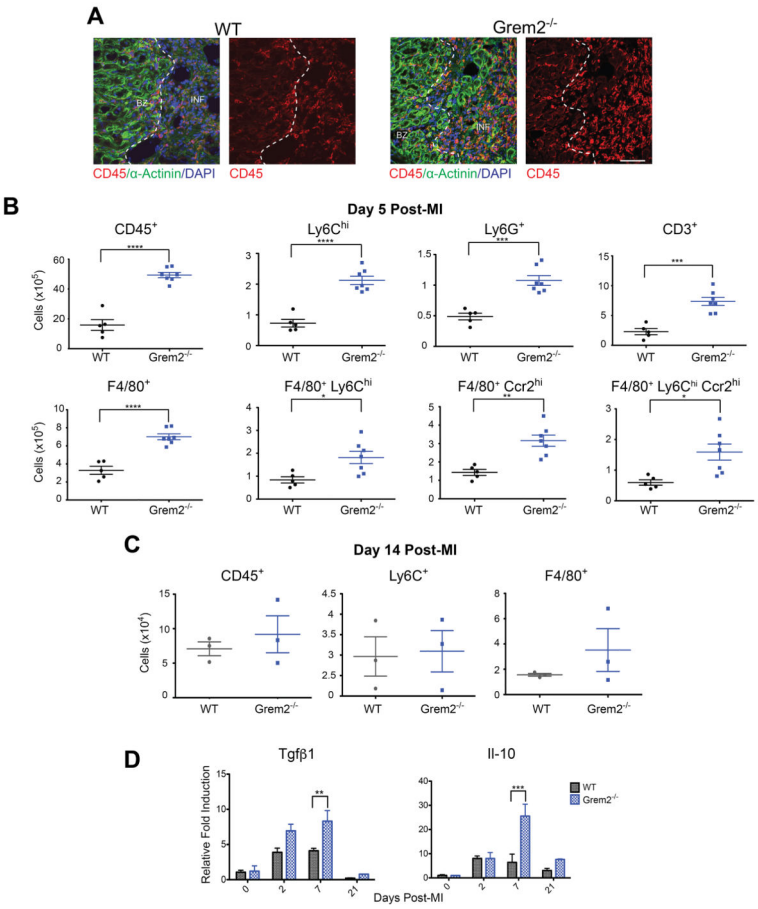

Figure 3. Loss of Grem2 increases the magnitude but not the duration of the inflammatory response after MI

(A) IF analysis at day 5 post-MI illustrates that *Grem2*$^{-/-}$ mice have increased levels of infiltrating leukocytes marked by CD45 (red) compared to *WT*s. α-Actinin (green) staining marks cardiomyocytes. DAPI marks cellular nuclei. Scale bars 50 μm. BZ=border zone, INF=infarct. **(B)** Flow cytometry analysis of single cell suspensions of non- cardiomyocyte cells isolated from whole hearts and analyzed using antibodies recognizing CD45, Ly6C, Ly6G, CD3, F4/80, and Ccr2 shows increased infiltration of inflammatory cells at day 5 post-MI in *Grem2*$^{-/-}$ mice compared to *WT*s. **P<0.05; **P<0.01; *** P < 0.001; ****P<0.0001*. Student's two-tailed unpaired *t*-test. *WT* N=5, *Grem2*$^{-/-}$ N=7. Bars represent means ± SEM. **(C)** Flow cytometry analysis of single cell suspensions of non-cardiomyocyte cells isolated from whole hearts of WT and *Grem2*$^{-/-}$ mice shows no significant differences of CD45^{+}, Ly6C^{+} and F4/80^{+} cells between the two groups at day 14 post-MI. N=3. **(D)** qPCR analysis of whole heart RNA samples isolated from *WT* and *Grem2*$^{-/-}$ mice at days 0, 2, 7 and 21 post-MI shows higher induction levels of *Tgfβ1* and *Il-10* in *Grem2*$^{-/-}$ hearts compared to *WT*s. *** P < 0.01; *** P < 0.001*. Two-way ANOVA with Bonferroni multiple comparisons test. N=3 per group for all time points. All data are means ± SEM. Abbreviations: *Il-10: Interleukin 10*.

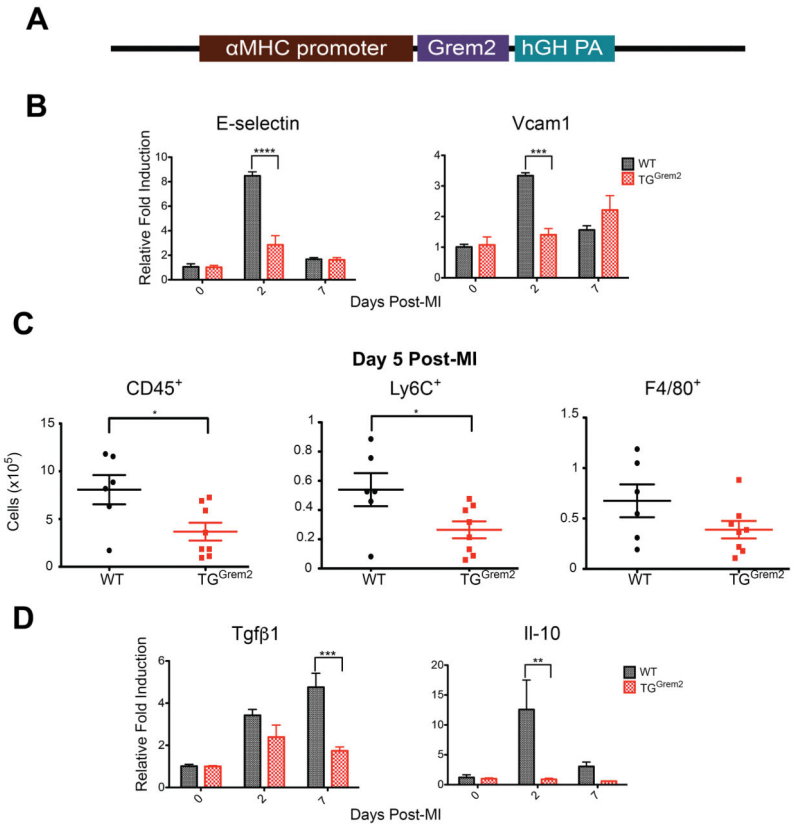

Figure 4. Grem2 overexpression attenuates inflammation after MI

(A) Schematic diagram of the DNA construct used to generate the *TG*^{Grem2} transgenic mice. The *Grem2* cDNA coding part was cloned behind a fragment of the *αMHC* (Myh6) gene promoter that specifically directs expression in adult cardiomyocytes. The construct includes the polyadenylation sequences of the human growth hormone gene (hGH PA). **(B)** qPCR analysis of whole heart RNA samples isolated from *WT* and *TG*^{Grem2} mice at days 0, 2, and 7 post-MI. Induction of endothelial cell-specific membrane proteins *E-selectin* and *Vcam1* is significantly attenuated in *TG*^{Grem2} hearts compared to *WT. *** P < 0.001; **** P < 0.0001.* Two-way ANOVA with Bonferroni multiple comparisons test. N=3 per group for all time points. All data are means ± SEM. **(C)** Flow cytometry analysis of single cell suspensions of non-cardiomyocyte cells isolated from whole hearts 5 days post-MI shows decreased number of CD45,$^{+}$ Ly6C^{+} and F4/80^{+} cells in *TG*^{Grem2} hearts compared to *WT. * P < 0.05.* Student's two-tailed unpaired *t*-test. *WT* N=6, *TG*^{Grem2} N=8. Bars represent means ± SEM. **(D)** qPCR analysis of whole heart RNA samples isolated from *WT* and *TG*^{Grem2} mice at days 0, 2, and 7 post- MI shows lower fold induction of *Tgfβ1* and *Il-10* in *TG*^{Grem2} hearts compared to *WT. ** P < 0.01; *** P < 0.001.* Two-way ANOVA with Bonferroni multiple comparisons test. N=3 per group for all time points. All data are means ± SEM.

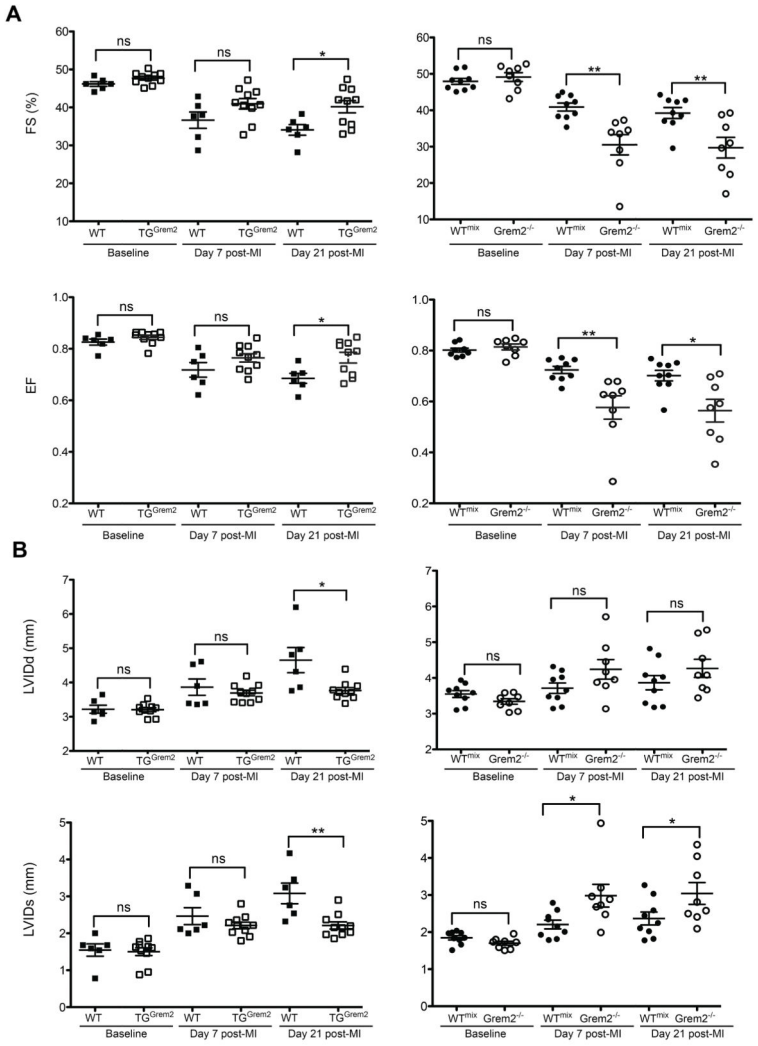

Figure 5. Grem2 improves cardiac function after MI

WT and TG^{Grem2} mice (both in C57BL/6 background), as well as WT^{mix} and $Grem2^{-/-}$ mice (both in mixed C57BL/6 and 129/Sv background) underwent permanent ligation of the LAD artery and cardiac dimensions were determined by echocardiography at several time points post-MI. **(A)** Fractional shortening (FS) and Ejection Fraction (EF) measurements at day 0 (baseline), 7, and 21 post-MI indicate cardiac function is improved in TG^{Grem2} mice compared to their *WT* siblings, whereas $Grem2^{-/-}$ mice exhibit worse cardiac function compared to WT^{mix} beginning at day 7 post-MI. **(B)** Improvement of cardiac function in TG^{Grem2} mice is due to preservation of both diastolic and systolic Left Ventricular Internal Diameter ($LVID_d$ and $LVID_s$) 21 days post-MI. Conversely, worsened function in $Grem2^{-/-}$ mice is mainly due to higher $LVID_s$ parameters as compared to WT^{mix} controls. *ns=not significant; * P < 0.05; **P < 0.01.* Student's two-tailed unpaired *t*-test. *WT* N=6, TG^{Grem2} N=10, WT^{mix} N=9, $Grem2^{-/-}$ N=8. Bars represent means ± SEM.

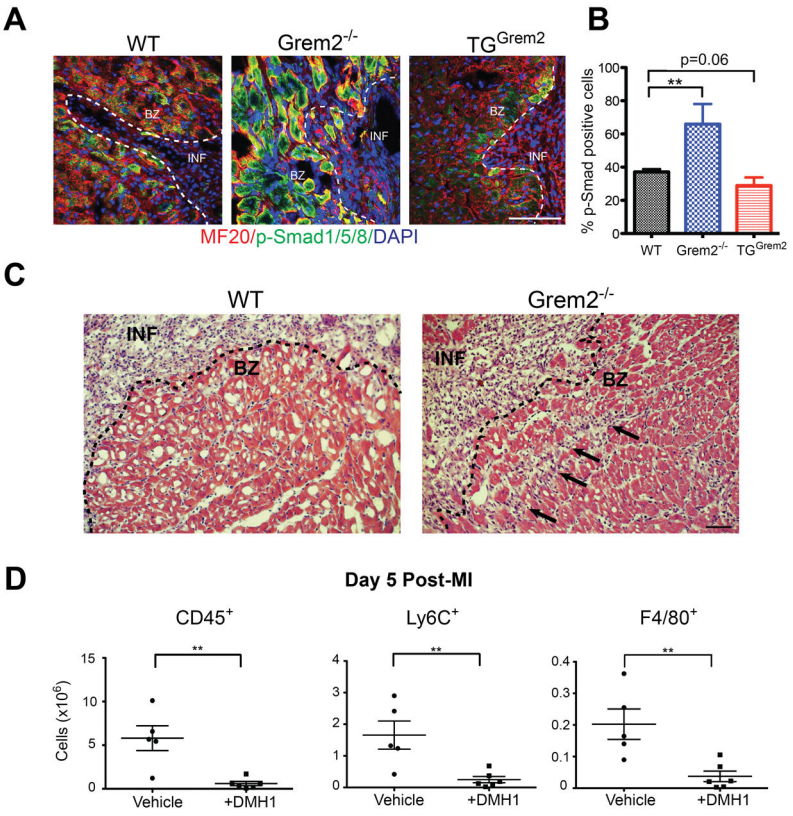

Figure 6. Grem2 regulates canonical/p-Smad1/5/8 BMP signaling in peri-infarct area cardiomyocytes

(A) IF analysis of cardiac tissue sections 7 days post-MI using antibodies recognizing p-Smad1/5/8 (green) and Myosin Heavy Chain (MF20, red) shows activation of canonical BMP signaling in cardiomyocytes in the peri-infarct border zone. DAPI marks cellular nuclei. The number of p-Smad1/5/8^{+} cardiomyoctyes is increased in *Grem2*$^{-/-}$ mice and decreased in *TG*^{Grem2} mice. Scale bars 100 μm. BZ=infarct border zone; INF=infarct. **(B)** Quantification of p-Smad1/5/8^{+} cells in the infarct border zone as percentage of total MF20^{+} cells per viewing area between *WT, Grem2*$^{-/-}$, and *TG*^{Grem2} mice. *** P < 0.01*. Student's two-tailed unpaired *t*-test. N=3. All data are means ± SEM. **(C)** Hematoxylin & Eosin staining 5 days post-MI shows that inflammatory cell infiltration (arrows) beyond the infarct border (dotted line) is greater in the *Grem2*$^{-/-}$ mice compared to *WT* counterparts. Scale bars 10 μm. BZ=border zone, INF=infarct. **(D)** *Grem2*$^{-/-}$ mice were injected once daily via IP with either the canonical BMP signaling inhibitor DMH1 or vehicle (DMSO) 2 days, 3 days, and 4 days post-MI. Number of total CD45^{+}, Ly6C^{+} and F4/80^{+} cells in whole hearts at 5 days post-MI were determined by flow cytometry. DMH1 injected mice have a decreased inflammatory cell infiltration compared to vehicle controls. *** P < 0.01*. Student's two-tailed unpaired *t*-test. Vehicle N=5, +DMH1 N=6. Bars represent means ± SEM.

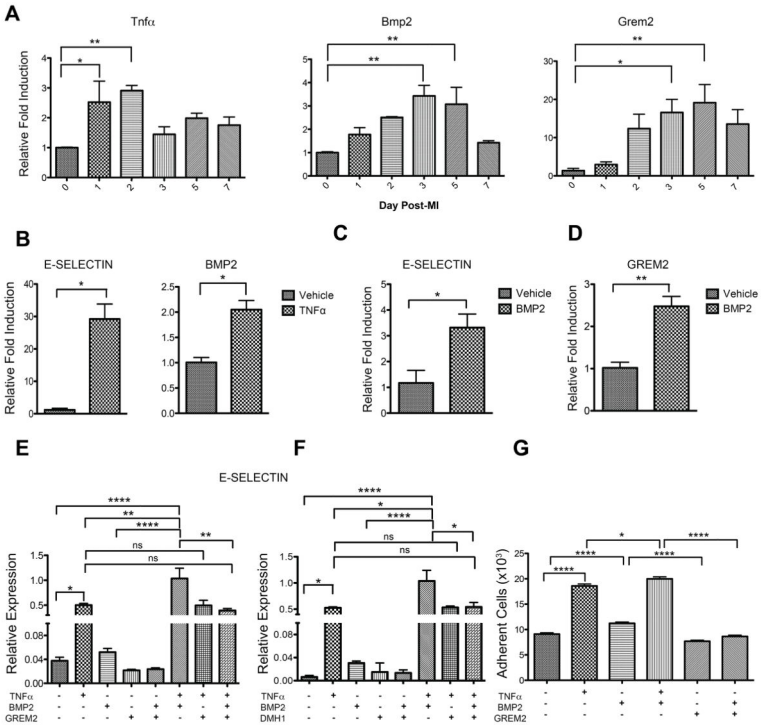

Figure 7. Grem2 inhibits the pro-inflammatory effect of BMP2 on endothelial cells

(A) qPCR analysis of whole heart RNA samples isolated from *WT* mice at days 0, 1, 2, 3, 5 and 7 post-MI shows sequential induction of *Tnfa, Bmp2* and *Grem2* during the cardiac repair process. ** P < 0.05; ** P < 0.01.* One-way ANOVA with Dunnett's multiple comparisons test. N=3 for all time points. All data are means ± SEM. **(B)** qPCR analysis of RNA samples isolated from Human Microvascular Endothelial Cells (HMEC) at 4 hours (left) and 24 hours (right) after TNFα treatment shows TNFα induces *E-SELECTIN* and *BMP2* expression. ** P < 0.05.* Student's two-tailed unpaired *t*-test. N=3 per group. All data are means ± SEM. **(C, D)** qPRC analysis shows BMP2 induces *E-SELECTIN* and *GREM2* in HMEC cells after 24 hours. ** P < 0.05; **P<0.01.* Student's two-tailed unpaired *t*-test. N=3 per group. All data are means ± SEM. **(E, F)** qPCR analysis of RNA sample isolated from HMEC 24 hours after treatment with TNFα, BMP2, Grem2 and DMH1 in different combinations as indicated. **(E)** TNFα and BMP2 together superinduce expression of *E-SELECTIN*. Grem2 specifically inhibits the BMP2 effect, but has no effect on the *E-SELECTIN* induction by TNFα. **(F)** Canonical BMP signaling inhibitor DMH1 specifically inhibits the BMP2-induced *E-SELECTIN. ns=not significant; * P < 0.05; ** P < 0.01; **** P < 0.0001.* One-way ANOVA with Dunnett's multiple comparisons test. N=3 for all treatments. All data are means ± SEM. **(G)** Adhesion of human monocytes (THP-1 cells) to HMEC cells was measured after HMEC cells incubation with TNFα, BMP2, or in combination for 24 hours. TNFα and BMP2 induce binding of endothelial cells to monocytes. Grem2 specifically inhibits the BMP2 effect. ** P < 0.05; **** P < 0.0001.* One-way ANOVA with Bonferroni's multiple comparison test. N=36. All data are means ± SEM.

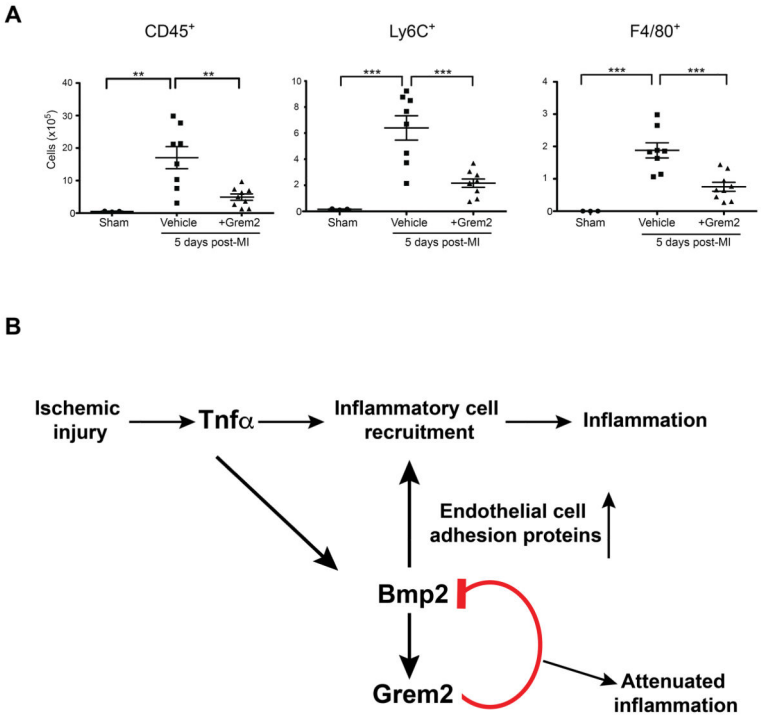

Figure 8. Systemic Grem2 protein administration attenuates inflammation after MI

(A) WT mice were injected once daily via IP with either Grem2 protein or vehicle (PBS) at day 2, 3, and 4 after MI. The number of $CD45^+$, $Ly6C^+$ and $F4/80^+$ cells in whole hearts was determined by flow cytometry at day 5 post-MI. Grem2 injected mice have decreased inflammatory cell infiltration compared to controls. *** P < 0.01; *** P < 0.001.* One-way ANOVA with Bonferroni multiple comparisons test. Sham N=3, Vehicle N=8, +Grem2 N=9. Bars represent means ± SEM. **(B)** Model of the role of Grem2 during the inflammatory phase after MI. Cardiomyocyte cell death after ischemic injury causes induction of TNFα, which directly stimulates expression of chemokines and endothelial membrane proteins to initiate inflammatory cell recruitment. TNFα also induces the expression of Bmp2 that further augments the pro-inflammatory phenotype of endothelial cells. Bmp2 in turn induces its own negative modulator Grem2 that inhibits the Bmp2-mediated inflammatory effects.